UCRL-51687

IN-SITU PERMEABILITY ANALYSIS USING BAROMETRIC PRESSURE FLUCTUATIONS

A. E. Sherwood

November 4, 1974

Prepared for U.S. Atomic Energy Commission under contract No. W-7405-Eng-48

LAWRENCE LIVERMORE LABORATORY

University of California/Livermore

Printed in the United States of America
Available from
National Technical Information Service
U.S. Department of Commerce
5285 Port Royal Road
Springfield, Virginia 22151
Price: Printed Copy $ * ; Microfiche $1.45

*Pages	NTIS Selling Price
1-50	$4.00
51-150	$5.45
151-325	$7.60
326-500	$10.60
501-1000	$13.60

TID-4500, UC-11
Environmental and Earth Sciences

LAWRENCE LIVERMORE LABORATORY
University of California/Livermore, California/94550

UCRL-51687

IN-SITU PERMEABILITY ANALYSIS USING BAROMETRIC PRESSURE FLUCTUATIONS

A. E. Sherwood

MS. date: November 4, 1974

Contents

IN-SITU PERMEABILITY ANALYSIS USING BAROMETRIC PRESSURE FLUCTUATIONS

Abstract

Methods of inferring in-situ permeability from measurements of barometric pressure fluctuations are reviewed. The technique has been used in air-saturated porous media at the Nevada Test Site. Possible application is discussed for a water-saturated coal outcrop. The underlying differential equation is derived and the requirements for linearity are shown, along with the conditions where the effect of gravity may be neglected. The analogy between pressure-wave propagation and signal propagation on an electrical transmission line is discussed. Transmission line methods are used to investigate reflections from the end of a finite path, leakage to the surroundings from permeable sidewalls, and the signal perturbations introduced by a sampling probe. A computer program is described to evaluate the response in radial flow to a step change in pressure. A comparison is made between pressure waves in radial and linear flow geometry.

Nomenclature

a	radius	m	V	complex voltage	V
A	area	m^2	w	fluctuation function, Eq. (6)	
C	capacitance/length	F/m	z	position coordinate	m
f	mass flux	$kg/m^2 \cdot s$	Z_o	characteristic impedance	Ω
F	integral defined by Eq. (A1)		α	gravity factor, Eq. (4)	l/m
g	gravitational acceleration	m/s^2	β	equation of state constant, Eq. (3)	$(s/m)^2$
$g(\xi,\tau,u)$	integrand defined by Eq. (A2)		β_ϱ	liquid compressibility, Eq. (3′)	1/Pa
G	conductance/length	S/m	γ	propagation constant	l/m
$h(\xi,u)$	function defined by Eq. (A3)		γ'	attenuation constant	1/m
i	current	A	γ''	phase constant	l/m
I	complex current	A	δ	permeability ratio	
j	$\sqrt{-1}$		Δp	pressure change	Pa
k	permeability	m^2	ϵ	pressure scale factor, Eq. (6) error term in Appendix	
ℓ	line length	m	ζ	dimensionless distance	
L	inductance/length	H/m	η	area ratio	
m	mass flowrate	kg/s	κ	diffusivity, Eq. (7)	m^2/s
N_o	function defined in Eq. (32)		κ_ϱ	liquid diffusivity, Eq. (7′)	m^2/s
p	pressure fluctuation	Pa	λ	wavelength	m
P	pressure	Pa	μ	viscosity	Pa·s
P_o	mean ambient pressure	Pa	ν	wavenumber, Eq. (21)	l/m
r	radial coordinate	m	ξ	r/a, dimensionless distance	
R	resistance/length	Ω/m	ρ	density	kg/m^3
s	sink term	$kg/m^3 \cdot s$	σ	gas mass transfer coefficient	l/s
t	time	s	σ_ϱ	liquid mass transfer coefficient	l/s
u	integration variable		τ	$\kappa t/a^2$, dimensionless time	
U	superficial velocity	m/s	ϕ	porosity	
v	voltage	V	ϕ_o	function defined in Eq. (32)	
v_p	propagation velocity	m/s	ω	angular frequency	rad/s

1. Introduction

The idea of using barometric pressure fluctuations to determine in-situ permeability was first suggested in a report by Morris and Snoeberger.[1] The method has been applied at the AEC Nevada Test Site to investigate the permeability of subsidence chimneys and near-surface alluvium. Chimneys are large, roughly cylindrical regions with radii in the 10-to-100-m range, and with a length/diameter ratio of about 6/1.[2] They are formed by subsidence of overlying strata into the cavity created by an underground nuclear explosion.[3]

The general idea is that naturally occurring barometric pressure fluctuations, impinging on the ground surface, will drive pressure waves down into the porous medium. If pressure is monitored over an extended time period, both at the surface and at some depth in the medium, it is possible to determine the diffusivity of the medium by an unsteady-state analysis. The idea is analogous to the determination of thermal diffusivity of near-surface rock, using thermal waves driven by seasonal surface temperature fluctuations.[4]

Subsequent reports on this subject discuss development of the pressure measurement and data handling systems. Several field tests have also been described, along with data and data analyses.[5-11] The next section of this report outlines and compares some different approaches to data analysis.

In Sec. 3, we give some needed attention to developing the basic mathematical model that will serve as the starting point for any method of data analysis. The underlying assumptions are spelled out and clarified.

Section 4 focuses on the analogy in linear flow between pressure wave propagation and signal propagation on an electrical transmission line. The conceptual and quantitative usefulness of transmission line theory is demonstrated by applying the method to a variety of problems. A possible application in a water-saturated coal seam that outcrops at the surface is discussed in Sec. 4.9.

There is current interest in radial pressure wave propagation from an open borehole into permeable surroundings. Section 5 describes a computer program to evaluate the radial flow response to a step change in pressure. A brief comparison is made between pressure wave propagation in linear and radial flow.

2. Data and Methods of Analysis

To get some feeling for the data analysis problem, it is helpful to look at some typical barometric pressure fluctuations. Figure 1 shows surface pressure data[6] on a highly expanded pressure scale covering a five-day period in May, 1972. One can see a semidiurnal (12 h) periodicity superimposed on a lower frequency weather front. The semidiurnal fluctuations are very small in amplitude, of the order of a few tenths percent of ambient pressure. The mean ambient surface pressure is about 86.2 kPa (12.5 psia).[12] Figure 2 shows surface pressure data[9] over the month of December, 1973. On this time scale, cyclic weather fronts of a few days duration are the dominant features. These oscillations are usually within ±2% of ambient

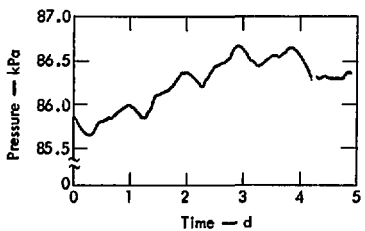

Fig. 1. Atmospheric pressure – Yucca Flat, Nevada, May, 1972.

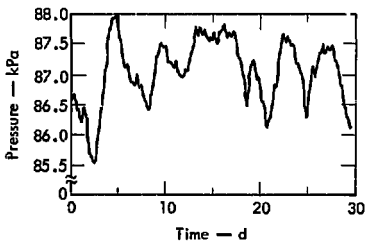

Fig. 2. Atmospheric pressure – Yucca Flat, Nevada, December, 1973.

pressure. Subsurface pressure measurements are similar in appearance to the figures shown except that the fluctuations are damped, with the higher frequency components being more severely attenuated.

The computational problem is to find the permeability of a porous region, given the measured surface pressure fluctuations that act as a boundary forcing function, and given the measured subsurface pressure response. As part of this problem, one has to develop a mathematical model for flow in the porous region and make assumptions about the geometry of the region. The equation to be solved, as will be shown in Secs. 3 and 4.3, is a dissipative pressure wave equation, effectively a time-dependent diffusion equation.

One method of attack is to assume trial values for permeability and then try to match the subsurface pressure response by solving the unsteady diffusion equation in finite diffence form.[7] This method is necessary if the geometry of the region is known to be complicated. An inherent disadvantage is the large amount of computer time spent finding the pressure response at all points in the medium, while the measured response is only available at one or, at most, a few points.

A more efficient approach is to carry out the pressure response matching with an analytical solution to the diffusion equation. This is possible if the geometry is simple and if the differential equation is linear, as shown in Sec. 3. The mathematical problem then reduces to superimposing particular solutions to the differential equation to represent the complicated boundary-forcing pressure displayed in Figs. 1 and 2. Two distinct methods have been used to date, one based on a decomposition of the surface pressure into square waves and the other on a decomposition into sinusoidal waves.

2.1 Square Wave Analysis

The method of square wave decomposition is sketched in Fig. 3. Measured surface pressure data points are used directly to define a sequential train of square waves. How well these represent the continuously changing surface pressure will depend on the spacing of the measurements. Each square wave is simply a rectangular pressure pulse that influences the boundary during a brief pulse interval. To solve the diffusion equation with a sequence of step changes as a boundary condition requires the use of Duhamel's superposition integral.[13]

Each rectangular pressure pulse can be considered to be made up of two step changes in pressure. With a linear geometry, the response in the porous medium to a boundary step change takes the form of an error function. The error function is an easily evaluated integral, and this linear model has been useful for data analysis.[9-11] Permeability estimates have been made, with an accuracy to about one significant figure, for several Nevada chimneys and near-surface alluvium. The response in radial flow to a step change in boundary pressure leads to a more complicated integral, which is discussed in Sec. 5.1.

The advantage of the square wave method is that it is the simplest possible way to represent a fluctuating boundary

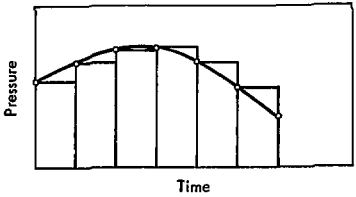

Fig. 3. Square wave approximation of barometric pressure measurements.

condition, and one can proceed immediately to the process of matching subsurface pressure response. The main disadvantage is that the surface pressure data is accepted at face value because there is no fitting or smoothing procedure to help reject spurious data points.

2.2 Sine Wave Analysis

Another way to represent the boundary pressure is with a Fourier series of sine and cosine waves of different frequency. This type of decomposition emphasizes the wave-like character of the fluctuations and is a natural approach, especially if periodic waves are present. Lindzen[14] has reviewed the history and current status of the theory of atmospheric pressure "tides". The theory predicts, and measurements confirm, that a periodic semidiurnal pressure tide will predominate in near-equatorial latitudes. In the mid-latitudes lower frequency pressure tides, or "weather fronts", are expected to dominate and to obscure the semidiurnal fluctuations. The Nevada measurements shown in Figs. 1 and 2 are consistent with this framework.

The diffusion equation for a porous region with simple geometry is easily solved for a periodic forcing function of given frequency (monochromatic). Given that the atmospheric pressure tide has been decomposed into a discrete frequency spectrum, then the subsurface pressure response can be calculated by a simple additive superposition of line spectrum components.

One virtue of this approach, which we will stress in Sec. 4, is simply the conceptual benefit of viewing flow in porous media as a wave propagation phenomenon.

Other advantages, which remain to be exploited, lie in the extra information inherent in a spectral analysis.[15] For example, most of the noise could be removed from the raw pressure data before starting the response matching process. Also, if permeability is to be deduced by a least-squares[11] or similar error criterion, it would be possible to see how the error is partitioned among spectral components.

The obvious disadvantage of harmonic analysis is the computational labor in determining Fourier coefficients. Also, the low frequency weather fronts are cyclic but not periodic.[8] A low "frequency" that appears on casual observation will tend to disappear upon Fourier decomposition into a broad line spectrum

3. Linearized Differential Equation

We start with the basic equations of mass and momentum conservation (Darcy's law)

$$\frac{\partial}{\partial t}(\phi\rho) + \vec{\nabla} \cdot \vec{f} + s = 0, \tag{1}$$

and

$$\vec{f} = \frac{-k\rho}{\mu}(\vec{\nabla}P - \rho\vec{g}), \tag{2}$$

where t is time, ϕ and k are porosity and permeability of the porous medium, and ρ, P, μ and $\vec{f}$ are gas (air) density, pressure, viscosity, and mass flux vector. The $\vec{g}$ vector points downward with the magnitude of gravitational force per unit mass. A sink term s, included for generality, allows for a mass removal rate per unit volume.

3.1 Gas-Saturated Media

If the fluid filling the pore space of the porous medium is a gas, we use the equation of state

$$\rho = \beta P, \tag{3}$$

where β is a proportionality constant for an isothermal gas.

Combining the equations above and carrying out the indicate operations, assuming that the physical properties ϕ, k, μ, and β are constant, gives

$$\phi\beta\frac{\partial P}{\partial t} = \frac{k\beta}{\mu}\left[P\nabla^2 P + |\vec{\nabla}P|^2 - \alpha\frac{\partial P^2}{\partial z}\right] - s, \tag{4}$$

where the constant α represents the effect of gravity,

$$\alpha \equiv \beta g,$$

and Eq. (4) holds for any geometry with z taken as a vertical coordinate increasing downward.

For a nonflowing vertical gas column, the solution to Eq. (4) is simply

$$P = P_0 e^{\alpha z},$$

where P_0 is the mean ambient surface pressure. For an ambient temperature air column, $\alpha \approx 1.2 \times 10^{-4}$ m^{-1} and the gravity correction is only about 2.4% at a depth of 200 m. However, even at a nominal 200-m depth, the gravity correction is several times larger than a typical pressure fluctuation.

A convenient way to nearly decouple the influence of gravity is to make the definition

$$P \equiv P_0 e^{\alpha z} + p, \tag{5}$$

where the first term represents the gravity effect, and p is a deviatory or fluctuation pressure. To aid in the linearization process and to emphasize that p is a small deviation from ambient pressure, it is helpful to define

$$p(\vec{r},t) \equiv \epsilon P_0 w(\vec{r},t), \tag{6}$$

where $w(\vec{r},t)$ is a fluctuation function that depends on spacial location $\vec{r}$ and time t, and which for now we will presume to be *sinusoidal* (see Eq. (22) for verification) with the function and its derivatives having an order of magnitude of unity. The scale factor ϵ relates the magnitude of the pressure fluctuation $p(\vec{r},t)$ to the mean ambient surface pressure P_0. As previously discussed, ϵ is always a small number, seldom larger than 10^{-2}.

Substituting Eqs. (5) and (6) into (4) gives

$$\frac{\partial w}{\partial t} = \kappa\epsilon^{\alpha z}(\nabla^2 w - \alpha^2 w) + \epsilon\kappa\left(w\nabla^2 w - \alpha\frac{\partial w^2}{\partial z} + |\vec{\nabla}w|^2\right)$$

$$- \frac{s}{\phi\beta P_0 \epsilon},$$

where κ is defined by

$$\kappa \equiv \frac{kP_0}{\phi\mu} \tag{7}$$

and may be considered a diffusivity since the units are (length)^2 (time)$^{-1}$. Since $\epsilon \ll 1$, the terms involving ϵ may be dropped giving

$$\frac{\partial w}{\partial t} = \kappa\epsilon^{\alpha z}(\nabla^2 w - \alpha^2 w) - \frac{s}{\phi\beta P_0 \epsilon}.$$

One now has a linear differential equation with slightly variable coefficients via the factor $\epsilon^{\alpha z}$ if the sink term is linear. Now $\alpha z = 1$ at a depth of about 8.3 km, so that $\alpha z \ll 1$ at ordinary depths of interest. Also $\alpha^2 w \ll \nabla^2 w$ because of our assumption that the function w and its derivatives are of the same order of magnitude. The equation for fluctuations then reduces simply to

$$\frac{\partial w}{\partial t} = \kappa \nabla^2 w - \frac{s}{\phi \beta P_o e},$$

and the function w, having served its purpose, can now be replaced by deviation pressure via the defining Eq. (6) to give

$$\frac{\partial p}{\partial t} = \kappa \nabla^2 p - \frac{s}{\phi \beta}.$$

The nature of the sink term s has not yet been specified. In a later section we will associate s with leakage through a slightly permeable boundary. For now, assume that the leak rate is proportional to the pressure deviation

$$\frac{s}{\phi \beta} \equiv \sigma p, \tag{8}$$

where σ is a constant, analogous to a mass transfer coefficient, whose magnitude will depend on external conditions. Using this definition,

$$\frac{\partial p}{\partial t} = \kappa \nabla^2 p - \sigma p. \tag{9}$$

In summary, Eq. (9) is a linear differential equation for the propagation of small gas pressure disturbances through a porous medium of arbitrary geometry. The equation is valid only for pressure fluctuations that are small compared to ambient pressure. Gravity affects the absolute pressure, but is effectively decoupled from the fluctuations by Eq. (5). The fluctuations will propagate without knowledge of gravity to considerable, but not unlimited, depths. The parameter of interest is the diffusivity κ that is directly related by Eq. (7) to the permeability and porosity of the porous medium.

3.2 Liquid-Saturated Media

For a liquid-saturated porous medium we replace Eq. (3) with the equation of state

$$\rho = \rho_o [1 + \beta_\ell (P - P_o)], \tag{3'}$$

where ρ_o is liquid density at ambient pressure P_o, and β_ℓ is liquid compressibility. The influence of gravity can again be decoupled by writing the analog to Eq. (5) for a liquid, i.e., defining the total pressure P at depth z as the hydrostatic pressure plus a small deviation pressure p:

$$P \equiv P_o + (e^{\rho_o \beta_\ell g z} - 1)/\beta_\ell + p. \tag{5'}$$

By carrying through the analysis of the last section and again dropping small terms, a diffusion equation in the same form as Eq. (9) results:

$$\frac{\partial p}{\partial t} = \kappa_\ell \nabla^2 p - \sigma_\ell p, \tag{9'}$$

when the diffusivity and leak rate for a liquid-saturated media are defined by

$$\kappa_\ell \equiv \frac{k}{\phi \mu \beta_\ell}, \tag{7'}$$

and

$$\frac{s}{\phi \rho_o \beta_\ell} \equiv \sigma_\ell p. \tag{8'}$$

Since Eqs. (9) and (9') have exactly the same form, the analytical discussion that follows applies to either gas- or liquid-saturated media. Specific calculations and parameter estimates, however, will be based on air as the saturating fluid, except in Sec. 4.9 where water will be considered.

4. Linear Propagation of Monochromatic Waves

In this section we will consider a one-dimensional (i.e., geometrically linear) form of Eq. (9) where the pressure fluctuation depends only on one coordinate, the vertical axis z, and where $\nabla^2 p$ simplifies to

$$\nabla^2 p = \frac{\partial^2 p}{\partial z^2}$$

This will be a model for vertical propagation from ground surface (z=o) into a permeable subsidence chimney region. We will use a sinusoidal monochromatic forcing function at the surface, specifically

$$p(z=o,t) = \epsilon P_o \cos(\omega t), \tag{10}$$

where ω is the angular frequency of the fluctuation.

The behavior of pressure fluctuations bears a close analogy to the propagation of signals on an electrical transmission line. Many of the ideas and results of transmission line theory can be used directly by properly interpreting the symbols.

4.1 The Electrical Transmission Line

The telegrapher's equations for the propagation of electrical potential v and current i along a distributed parameter transmission line are given by[16,17]

$$-\frac{\partial v}{\partial z} = Ri + L\frac{\partial i}{\partial t}, \qquad (11a)$$

and

$$-\frac{\partial i}{\partial z} = Gv + C\frac{\partial v}{\partial t}, \qquad (11b)$$

where R,L,G, and C are line parameters. Series and shunt resistance are represented by R and G, series inductance by L, and shunt capacitance by C, and the parameters are all expressed per unit length of line. A wave equation for either v or i is obtained by appropriate differentiation and combination of the above pair of equations.

For v, the result is

$$(LC)\frac{\partial^2 v}{\partial t^2} + (RC + LG)\frac{\partial v}{\partial t} = \frac{\partial^2 v}{\partial z^2} - (RG)v. \qquad (12)$$

As might be suspected, electrical potential v is analogous to pressure fluctuation p. One can see a resemblance between Eq. (12) and the l-d form of Eq. (9), although the pressure equation seems to lack a second-time derivative term equivalent to $LC\frac{\partial^2 v}{\partial t^2}$ in Eq. (12).

As a matter of fact, such a term should be present in the equations for both mass flow and heat flow, although it is neglected ordinarily.

Transmission lines are often nearly "lossless" (R=G=0), in which case Eq. (12) reduces to an undamped wave equation

$$LC\frac{\partial^2 v}{\partial t^2} = \frac{\partial^2 v}{\partial z^2},$$

where the propagation velocity of a wavefront ("phase" velocity) is a constant $1/\sqrt{LC}$, which is a little less than the velocity of light in free space and independent of the impressed signal frequency. For a "lossy" line (R,G > 0), the propagation velocity is frequency dependent and less than the limiting value $1/\sqrt{LC}$.

4.2 The Fourier/Darcy Paradox

In Fourier's law for heat flux, the absence of an inductance term like $L\frac{\partial i}{\partial t}$ in Eq. (11a) gives rise to the so-called Fourier paradox, when an impulse or step change signal is impressed on a medium.[18,19] An impulse may be decomposed into a continuous frequency spectrum and that part of the spectrum where $\omega \to \infty$ will propagate with velocity $\to \infty$. Thus, an impulse is "felt" instantaneously at a remote location in the medium. The paradox is removed by adding a time-dependent term to Fourier's law and the magnitude of the equivalent thermal inductance has been estimated by Chester.[19] The result is to limit thermal propagation velocity to essentially the speed of sound in the medium.

There is a similar paradox in the usual form of Darcy's law for mass flux, although I am not aware of any discussions in the literature on the "Darcy paradox". Based on a theoretical analysis of flow in microscopic channels, Irmay[20] derived an extended form of Darcy's law that includes both a time-dependent term and a high flowrate correction. His main purpose was to find a correction term for Darcy's law for high flowrates, and he chose to ignore the inductance term.

4.3 Mass-Flow Analogy

For the purpose of showing the mass-flow/electrical-flow analogy, we ignore Irmay's high flowrate correction and keep his inductance term to get the modified Darcy law

$$-\left(\frac{\partial P}{\partial z} - \rho g\right) = \frac{\mu}{\kappa} U + \frac{\rho}{\phi}\frac{\partial U}{\partial t}, \qquad (13)$$

where $U \equiv \frac{f}{\rho}$ is the superficial flow velocity.

If the time-dependent term is omitted from Eq. (13), it reduces to the l-d form of Darcy's law that is implied by Eq. (2). We now carry out a linearization procedure using Eq. (13) instead of Eq. (2), and this time developing a pair of equations for pressure fluctuation p and mass flowrate m,

$$m \equiv fA,$$

where A is the cross sectional area. We will omit the details, since the linearization approximations have been carefully outlined in the last section. The resulting pair of equations are:

$$-\frac{\partial p}{\partial z} = \left(\frac{\mu}{kP_o A\beta}\right) m + \left(\frac{1}{\phi A}\right)\frac{\partial m}{\partial t}, \qquad (14a)$$

and

$$-\frac{\partial m}{\partial z} = (\phi A c\beta)\, p + (\phi A\beta)\frac{\partial p}{\partial t}, \qquad (14b)$$

which are the fluctuating gas flow equivalent to the telegrapher's Eqs. (11a) and (11b). The analogy is complete; $p \Leftrightarrow v$, $m \Leftrightarrow i$, and the bracketed mass flow parameters in Eq. (14) can be directly associated with the corresponding line parameter R, L, G, and C in Eq. (11), as shown in Table 1. A similar pair of equations can be developed for small fluctuations in liquid flow, and the corresponding parameters are also listed in Table 1. The pressure wave equation obtained by combining Eqs. (14a) and (14b) is

$$\beta \frac{\partial^2 p}{\partial t^2} + (1/\kappa + \beta\sigma) \frac{\partial p}{\partial t} = \frac{\partial^2 p}{\partial z^2} - (\alpha/\kappa)\, p, \qquad (15)$$

which is directly comparable to Eq. (12).

For a hypothetical dissipationless medium ($\kappa \to \infty$, $\sigma \to 0$), the above reduces to an undamped wave equation where disturbances propagate at the limiting velocity $1/\sqrt{\beta}$, which is a little less than the adiabatic sound speed. This result is not surprising, but it is interesting to show how it follows from a suitable extension of Darcy's law.

One can formally "turn-off" the inductance effect by pretending that the sound speed is very large ($\beta \to 0$); Eq. (15) will then reduce to a 1-d version of our previously derived Eq. (9). Since we are dealing with a highly dissipative porous media where propagation velocity is usually constrained to a very small fraction of the sound speed, Eq. (15) reduces to Eq. (9) for all practical purposes.

Having shown the close analogy between pressure wave and electrical wave propagation, we next outline the solution procedure for the wave equation using the more compact electrical symbols and then return to mass flow for example applications.

Table 1. Corresponding variables of an electrical transmission line and pressure fluctuations in a porous medium.

	Mass flow parameter	
Electrical parameter	Gas saturated medium	Liquid saturated medium
v	p	p
i	m	m
R	$\frac{\mu}{kP_0A\beta}$	$\frac{\mu}{kA\rho_0}$
L	$\frac{1}{\phi A}$	$\frac{1}{\phi A}$
G	$\phi A\beta\sigma$	$\phi A\rho_0\beta_\ell\sigma_\ell$
C	$\phi A\beta$	$\phi A\rho_0\beta_\ell$
RC	$\frac{\beta}{\kappa}$	$\frac{1}{\kappa_\ell}$
RG	$\frac{\sigma}{\kappa}$	$\frac{\sigma_\ell}{\kappa_\ell}$
LG	$\beta\sigma$	$\rho_0\beta_\ell\sigma_\ell$
LC	β	$\rho_0\beta_\ell$

4.4 Solution to the Wave Equation[16,17]

To solve Eq. (12) for a monochromatic wave with frequency ω, assume that the instantaneous voltage v (z,t) is given by

$$v(z,t) = \mathrm{Re}\left[V(z)\, e^{j\omega t}\right], \qquad (16)$$

where V (z) is a function only of z and $e^{j\omega t}$ is the complex exponential function. The operation of Re[ ] means to take the real part of the bracketed expression, and this is performed when determining integration constants and again after the unknown function V (z) is determined. V (z) is often loosely referred to as voltage, but the reader should remember that the real space-time varying voltage is defined by Eq. (16). The above assumption converts the wave equation into an ordinary differential equation for V (z) so that

$$\frac{d^2V}{dz^2} - \gamma^2 V = 0,$$

where γ is called the propagation constant

$$\gamma = \sqrt{(R + j\omega L)(G + j\omega C)}. \qquad (17)$$

A split of γ into real and imaginary parts may be made so that

$$\gamma = \gamma' + j\gamma''$$

and, following Waldron[17],

$$2(\gamma')^2 = (RG - \omega^2 LC) + \sqrt{(RG - \omega^2 LC)^2 + (\omega RC + \omega GL)^2}, \qquad (17a)$$

and

$$2(\gamma'')^2 = -(RG - \omega^2 LC) + \sqrt{(RG - \omega^2 LC)^2 + (\omega RC + \omega GL)^2}. \qquad (17b)$$

The real part γ' gives the rate of decay of amplitude on a lossy line and is called the attenuation constant. The phase constant γ'' gives the phase shift of the signal relative to the input end of the line.

The solution of the equation for V (z) is

$$V(z) = V_1 e^{-\gamma z} + V_2 e^{\gamma z}, \qquad (18)$$

where V_1 and V_2 are integration constants, that may be complex numbers.

If current i is expressed in a form similar to Eq. (16)

$$i(z,t) = \mathrm{Re}\left[I(z) e^{j\omega t}\right], \qquad (19)$$

then the space dependent function I(z) can be expressed by

$$I(z) = \frac{V_1 e^{-\gamma z} - V_2 e^{\gamma z}}{Z_o} . \qquad (20)$$

where V_1 and V_2 are the same constants as in Eq. (18) and Z_o is called the characteristic impedance

$$Z_o = \sqrt{\frac{R + j\omega L}{G + j\omega C}} .$$

If the characteristic impedance is split into real and imaginary parts, one finds that the imaginary part contributes an additional phase shift for the current relative to the voltage at a given location on the line.

With this brief review of transmission line theory and terminology, we turn next to some applications.

4.5 The Long Vertical Line

Returning to pressure wave propagation, the simplest model is the case of a long (semi-infinite) vertical path without leakage (G=0) or inductance (L=0). The constant V_2 in Eq. (18) is zero since the disturbance must remain finite as $z \to \infty$. Using Eq. (16) and the boundary condition of Eq. (10),

$$V_1 = \epsilon P_o$$

and, therefore, $V(z) = \epsilon P_o e^{-\gamma z}$.

Translating the line parameters R and C in Eq. (17) into mass flow symbols give

$$\gamma = \sqrt{\frac{j\omega}{\kappa}} .$$

The complex propagation constant γ can also be expressed by

$$\gamma = \nu(1 + j),$$

where

$$\nu = \sqrt{\frac{\omega}{2\kappa}} \qquad (21)$$

and ν can be interpreted as a wavenumber. Using Eq. (16) again to find the real part of the pressure fluctuation, one finds

$$p(z,t) = \epsilon P_o e^{-\nu z} \cos(\omega t - \nu z). \qquad (22)$$

Equation (22) represents a propagating, damped pressure wave. The wave decays exponentially and has a phase lag νz that is proportional to the distance traveled. The wavelength on the line is

$$\lambda = \frac{2\pi}{\nu} = 2\pi\sqrt{\frac{2\kappa}{\omega}} , \qquad (23)$$

The propagation ("phase") velocity, i.e. the velocity at which a moving observer will notice no time variations in pressure, is

$$v_p = \frac{\omega}{\nu} = \sqrt{2\omega\kappa} . \qquad (24)$$

Now the main virtue of this model is that it gives a quantitative and easily visualized picture of the behavior of a surface barometric fluctuation as it progresses into the porous medium.

Suppose we take a fluctuation with a 24 period T, then the *angular frequency* ω is

$$\omega = \frac{2\pi}{T} = 7.27 \times 10^{-5} \text{ rad/s.}$$

Assuming representative values for porous media and gas properties:

$$k = 4.93 \times 10^{-11} \text{ m}^2 \text{ (50 darcy)},$$

$$\phi = 0.3,$$

$$P_o = 86.2 \text{ kPa (12.5 psia)},$$

and

$$\mu = 18\mu \text{ Pa·s (0.018 cp)}$$

giving a diffusivity, from Eq. (7), of

$$\kappa = 0.788 \text{ m}^2/\text{s}.$$

From ω and κ, the wavenumber, wavelength, and propagation velocity are:

$$\nu = 6.79 \times 10^{-3} \text{ m}^{-1},$$

$$\lambda = 925 \text{ m} ,$$

and

$$v_p = 38.5 \text{ m/h}.$$

Thus a fluctuation with a 24-h period propagates slowly, has a rather long wavelength, and is damped by a factor of 10 at depth

$$z = \frac{\ell n(10)}{\nu} \simeq 340 \text{ m}.$$

Lower frequency pressure fluctuations caused by gradual weather changes will penetrate the medium more slowly and with less damping than higher frequency fluctuations, which tend to damp out quickly.

4.6 The Finite Line

Since the permeable regions under investigation are not infinite in extent, one can ask how much error is introduced by this assumption when measurements are made in a given finite region. Transmission line theory provides an exact answer and a simple rule-of-thumb answer.

Both constants are needed in Eq. (18) if the line has a finite length ℓ. One is determined, as usual, by the forcing function at $z = 0$. The other is determined by the "open-circuit" condition $I = 0$ in Eq. (20), since there is no mass flow at $z = \ell$. This leads to

$$V(z) = cP_0 e^{-\gamma z}\left[\frac{1 + e^{-2\gamma d}}{1 + e^{-2\gamma \ell}}\right], \qquad (25)$$

where d is the distance from the end of the line to the measurement point z, i.e., $z + d = \ell$ as sketched in Fig. 4. If ℓ and d are very large, the bracketed expression above approaches unity and the remaining portion is the long-line result of the last section.

Converting the above equation for a finite line into real form is algebraically tedious, and the finite length affects both amplitude and phase shift relative to the same wave on an infinite line.

Basically, there are two types of errors. The first depends on the absolute length of the line, ℓ, and the second on how close one is measuring to the end of the line, d. In the first case, the error is roughly $\exp(-4\pi\ell/\lambda)$, and in the second case it is about $\exp(-4\pi/\lambda)$. For example, if d is a quarter-wavelength or more, the assumption of an infinite line is in error by about 4% ($\exp(-\pi) \approx 0.04$) or less.

As discussed earlier, the characteristic wave length λ is frequency and permeability dependent,

$$\lambda \propto \left(\frac{\kappa}{\omega}\right)^{1/2}.$$

and for the values of the parameters previously chosen

$$\frac{\lambda}{4} \approx 200 \text{ m}.$$

4.7 The Long Line with Leakage

On an electrical transmission line the shunt resistance G is a known parameter of the system. We have been carrying along the analogous mass sink term in Eq. (14b) to estimate the effect of leakage to the external environment from slightly permeable sidewalls of a subsidence chimney. In reality, one has a complicated 2-d flow problem, and we will make several simplifying assumptions to make a quantitative estimate of the leak rate.

First of all, assume that the external leakage region extends to infinity and has a finite permeability in the horizontal plane, but zero permeability in the vertical z direction. One can imagine that the external region consists of many thin horizontal layers with impermeable interfaces between them, as sketched in Fig. 5. The effect of this assumption will be discussed later.

Assume also that the flow is linear in the external region. If the chimney is cylindrical one would expect diverging radial flow; linear flow implies that the effective penetration depth is small. This assumption is optimistic in the sense that leakage will be underestimated.

Our assumptions have made the leak path itself equivalent to an electrical transmission line, and the method discussed in Sec. 4.4 can be used to find the current (leakage flux X area) at the external leak path boundary in terms of the impressed voltage (pressure fluctuation). The resulting current is directly

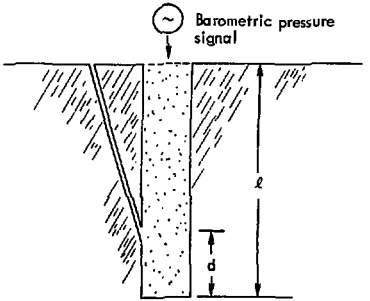

Fig. 4. Subsidence chimney of length ℓ, with distance d from measurement depth to end of permeable region.

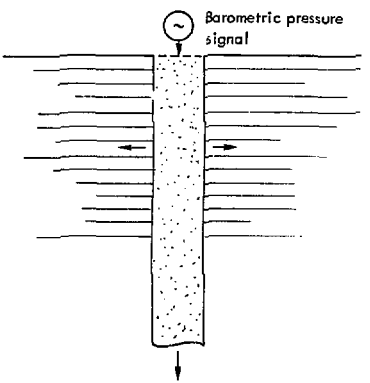

Fig. 5. Subsidence chimney viewed as a long transmission line with leakage.

proportional to voltage if one neglects a phase lag of $\pi/4$ rad. To put this assumption another way, the root-mean-square current and voltage are directly proportional to each other, and we assume the same relation for the instantaneous values. In mass flow terms, the external leakage flux f_e is related to pressure fluctuation p by

$$f_e = \phi_e \beta (\omega \kappa_e)^{1/2} p,$$

where ϕ_e and κ_e are the external leak path porosity and diffusivity. The mass leakrate per unit volume, s of Eq. (1), is related to f_e by

$$s = \frac{2}{a} f_e,$$

where 2/a is the surface area/volume ratio for a cylinder of radius a.

By comparing the above equations with Eq. (8), one finds that the mass transfer coefficient σ can be written

$$\sigma = \frac{2}{a} (\delta \omega \kappa)^{1/2} \quad , \tag{26}$$

where, for convenience, a leakage parameter δ has been introduced:

$$\delta \equiv \frac{k_e \phi_e}{k \phi} \quad . \tag{27}$$

If the external porosity ϕ_e and chimney porosity ϕ have about the same value, then δ is essentially the permeability ratio of the external medium to the subsidence chimney region.

At first thought, all we seem to have done is replaced an unknown mass transfer coefficient σ by an unknown permeability ratio δ. The point, however, is that the frequency dependence of σ has been spelled out, and we can now investigate how small the permeability ratio must be for typical fluctuation frequencies to avoid significant error.

The expression for V (z) is, as in Sec. 4.5 for the long line without leakage,

$$V(z) = \epsilon P_0 e^{-\gamma z},$$

but now the propagation constant γ includes the mass transfer coefficient σ. From Eq. (17) and Table 1

$$\gamma = \left(\frac{\sigma}{\kappa} + j \frac{\omega}{\kappa} \right)^{1/2} .$$

Splitting γ into attenuation constant γ' and a phase constant γ'', as in Sec. 4.4,

$$\gamma' = \nu \left(\frac{\sigma}{\omega} + \sqrt{1 + \left(\frac{\sigma}{\omega}\right)^2} \right)^{1/2} ,$$

and

$$\gamma'' = \nu \left(\frac{\sigma}{\omega} + \sqrt{1 + \left(\frac{\sigma}{\omega}\right)^2} \right)^{1/2} ,$$

where ν is the wavenumber defined by Eq. (21). One can see that the attenuation increases and the phase shift decreases for small but finite leakage.

Focusing on the attenuation, suppose we decided to estimate the permeability of the subsidence chimney region from the observed attenuation at some depth of a given frequency fluctuation. Using a propagation model without leakage ($\sigma = 0$) will give what we will call an "apparent" permeability. Using the model with leakage ($\sigma > 0$) will give a different value, which we will call the "true" permeability. From the above equation for γ', one can see that

$$\left(\frac{\text{apparent permeability}}{\text{true permeability}} \right) = \left(\frac{\sigma}{\omega} + \sqrt{1 + \left(\frac{\sigma}{\omega}\right)^2} \right)^{-1/2} ,$$

and from our leakage model

$$\frac{\sigma}{\omega} = \frac{2}{a} \left(\frac{\delta \kappa}{\omega} \right)^{1/2} .$$

The model tells us that apparent/true permeability is affected by a, κ, ω, and δ. Since the main question is the magnitude of the leakage parameter δ (external/true permeability), we use a nominal value of 25 m for chimney radius a, along with the representative values for κ and ω from Sec. 4.5, to give

$$\frac{\sigma}{\omega} \simeq 8.33\, \delta^{1/2} .$$

Figure 6 shows apparent/true permeability plotted as a function of δ. The figure shows that δ must be very small before leakage can be safely neglected in calculations. Even with $\delta = 10^{-2}$, the apparent calculated permeability is too low by about a factor of two. Figure 6 also shows the error caused by our assumption of zero vertical external permeability. If the external permeability is very small, barometric disturbances impinging on this region from ground surface will be quickly damped out, and the external region at a reasonable depth will not feel these direct waves. In this case, the assumption of zero vertical permeability is reasonable and somewhat conservative. If, on the other hand, the external permeability is nearly the same as the chimney permeability, external waves of significant magnitude will propagate from ground surface to depth and will tend to buffer and impede leakage. If $\delta = 1$, there will, of course, be no leakage at all. The dotted curve in Fig. 6 has been drawn freehand to indicate qualitatively what might be expected from a more correct 2-d leak model.

The main point of this section has been to develop an approximate leakage model that is valid for $\delta \ll 1$. The calculations indicate that large errors may result from neglecting leakage unless the external permeability is very small. Independent measurements of the surrounding environmental permeability are needed to resolve the question of leakage.

Additional information results from making simultaneous pressure measurements at several depths. If the external environment were understood, then this additional information

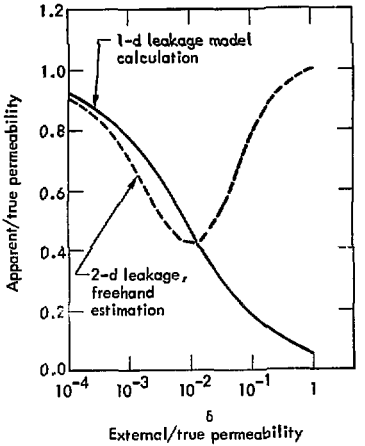

Fig. 6. Apparent/true permeability ratio as a function of leakage parameter δ.

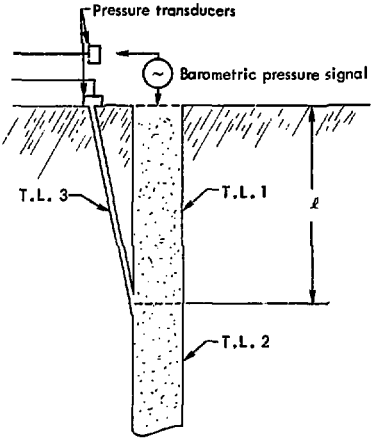

Fig. 7. Subsidence chimney and sensing line viewed as three transmission lines with a common junction point.

could be used to deduce possible vertical variations in chimney permeability.

4.8 Sampling Probe Effects

We will consider the effect of the finite volume (length and cross section) of the downhole sensing line or "sampling probe". Pressure fluctuations are not measured at depth, but instead by a transducer on the surface that is coupled downhole by a separate borehole. The question is how much does the signal measured at the top end of the sampling line differ from an unperturbed signal at depth?

Transmission line theory provides a ready answer if we consider that the system consists of three transmission lines with a common junction at depth as sketched in Fig. 7. Lines 1 and 2 are really part of the same line and have the same line parameters. Line 1 is of finite length ℓ, while line 2 is assumed to be a long line. Line 3 will have about the same length as line 1, but has different line parameters since it represents a wide open hole. We assume leak-free lines with no inductance.

Using the ideas in Sec. 4.4, one writes down the equations for voltage and current on each of the three lines and then has six constants of integration to determine. Three are found by using known conditions at the end of each line: line 1 has the driving signal impressed on the inlet end, line 2 is infinite which eliminates a constant, and line 3 is open-circuited ($I = 0$) at the ground surface end. At the junction point there are two independent equations expressing equality of voltage. The final condition is Kirchoff's law, stating that the algebraic sum of currents flowing into a circuit junction point equals zero. Omitting the algebra, the expression for (complex) voltage V_3 at the ground surface end of the sampling line is

$$V_3 = \frac{\epsilon P_o e^{-\gamma_3 \ell} \operatorname{sech}(\gamma_3 \ell)}{1 + \dfrac{Z_o}{2Z_{03}}(1 - e^{-2\gamma_3 \ell}) \tanh(\gamma_3 \ell)} , \qquad (28)$$

where sech and tanh stand for hyperbolic secant and tangent, and γ_3 and Z_{03} are the propagation constant and characteristic impedance of the sampling line.

Now this equation may appear a little opaque, but it becomes transparent on considering the magnitude of $\gamma_3 \ell$. The equivalent permeability, k_3, of the open sampling tube is very large[21] and in laminar flow is approximately $(a_3)^2/8$, where a_3 is the sampling tube radius. If we take $a_3 = 0.125$ m (a 9 7/8-in.-dia. borehole) and $\ell = 200$ m, then with our previous parameter values for ω, etc.,

$$\gamma_3 \ell = \nu_3 \ell (1 + j) \simeq 3.94 \times 10^{-4} (1 + j),$$

a very small number. Now $\gamma_3 \propto a_3^{-1}$, and so $\gamma_3 \ell$ is small even for a 1-mm tube.

The term sech $(\gamma_3 \ell)$ in Eq. (28) represents attenuation and phase lag along the sampling tube, and for $\gamma_3 \ell \ll 1$

$$\text{sech}\,(\gamma_3 \ell) \simeq 1 - \frac{(\gamma_3 \ell)^2}{2} + \ldots ,$$

$$\simeq 1 - 1.6 \times 10^{-7} j \quad .$$

Therefore, the signal is attenuated and phase-shifted to a negligible extent in passage through an open tube of reasonable size.

We should mention that the propagation velocity in the tube turns out to be about 37 m/s, which is about three orders of *magnitude larger than the main line but still well below sound* speed. This justifies the assumption of an inductance-free line.

The complicated term in the denominator of Eq. (28) corresponds, in an electronic sense, to loading down the circuit with a finite impedance sampling probe. We can neglect the factor $e^{-2\gamma\ell}$ since, for the main line parameter values, $2\gamma\ell \simeq 2.8\,(1+j)$.

The impedance ratio term can be written

$$\frac{Z_0}{2Z_{03}} = \eta \frac{\gamma}{\gamma_3} \quad ,$$

where in mass flow symbols

$$\eta \equiv \frac{A_3}{2\phi A} \quad ,$$

and A_3 and A are probe and main line cross sectional area. Since, for $\gamma_3 \ell \ll 1$

$$\tanh\,(\gamma_3 \ell) \simeq \gamma_3 \ell + \ldots ,$$

the denominator of Eq. (28) becomes

$$1 + \eta\gamma\ell + \ldots \quad .$$

Now, for our nominal tube and chimney radii of 0.125 m and 25 m, η is also a very small number ($\approx 4.2 \times 10^{-5}$) and therefore

$$1 + \eta\gamma\ell \simeq e^{\eta\gamma\ell} \quad .$$

Equation (28) then reads simply

$$V_3 \simeq \epsilon P_0\, e^{-\gamma\ell(1+\eta)} \quad ,$$

and by putting in the time factor and converting to real form with Eq. (16)

$$p_3 \simeq \epsilon P_0\, e^{-\nu\ell(1+\eta)} \cos\,[\omega t - \nu\ell(1+\eta)] \quad . \qquad (29)$$

By comparing with the long line Eq. (22) we see that the measured pressure fluctuation p_3 differs in amplitude and phase lag from the unperturbed value by the correction factor $(1+\eta)$. *Since η is so small, the correction* is negligible. The sampling tube would have to be about 6 m in radius before the correction amounts to 10%.

The sampling probe can range in size from a capillary tube to a large sewer pipe and still not cause significant error. The probe acts like a good electronic probe; it passes *the signal undistorted* to the measurement point and, because of the high impedance, it does not load down the circuit to be measured.

4.9 Water-Saturated Media and the Air/Water Interface

The discussion thus far has centered on what can be done *with pressure fluctuations impinging* at the ground surface on a rather permeable air-filled subsidence chimney. Another application of interest would be to measure the permeability of a steeply dipping coal seam that outcrops on the surface. A primary requirement is that the coal seam is isolated, i.e., bounded by less penneable surroundings.

For the coal seam, assume that permeability and porosity are:

$$k = 9.87 \times 10^{-14}\ \text{m}^2\ (0.1\ \text{darcy}) ,$$

and

$$\phi = 0.1$$

As a basis for comparison, assume the coal seam is dry (air saturated). Using Eq. (7) with the properties of air listed in Sec. 4.5 gives a diffusivity of

$$\kappa = 4.73 \times 10^{-3}\ \text{m}^2/\text{s}.$$

For a 24-h fluctuation period, using the long line equations of Sec. 4.5, the wavenumber, *propagation* velocity, and distance to decay by a factor of 10 are:

$$\nu = 8.8 \times 10^{-2}\ \text{m}^{-1} ,$$

$$v_p = 3.0\ \text{m/h} ,$$

and

$$z = 26\ \text{m}.$$

Note that the air diffusivity is small and that 26 m is not a very useful penetration depth.

In the more likely circumstance of a water-saturated coal *seam*, assume that water compressibility and viscosity are:

$$\beta_\ell = 4.93 \times 10^{-10}\ \text{Pa}^{-1}\ (5 \times 10^{-5}\ \text{atm}^{-1}) ,$$

and

$$\mu = 10^{-3}\ \text{Pa·s}\ (1\ \text{cp}).$$

The diffusivity from Eq. (7') is

$$\kappa_\ell = 2.00\ m^2/s,$$

which is a reasonably large number even for the (assumed) low permeability coal seam and is caused by the low compressibility of water as compared to air, which more than compensates for the higher viscosity of water. For a 24-h fluctuation period, the wavenumber, propagation velocity, and distance to decay by a factor of 10 are:

$$\nu = 4.3 \times 10^{-3}\ m^{-1},$$

$$v_p = 61\ m/h,$$

and

$$\ell = 540\ m.$$

A pressure fluctuation should, therefore, be detectable at a substantial depth in a water-saturated coal seam.

Another question that comes to mind is the effect of an air/water interface. If the water table is reasonably close to the surface, the attenuation per se in a short air column will not be bothersome but one might suspect poor coupling (a large impedance mismatch) at the interface, analogous to the large acoustic impedance mismatch between air and water. This turns out to be untrue, as can be shown by using the equation for characteristic impedance given in Sec. 4.4 (taking L=G=0) along with gas and liquid mass flow parameters of Table 1. The characteristic impedance ratio works out as:

$$\frac{(Z_o)\ \text{water}}{(Z_o)\ \text{air}} = \frac{[(\mu/\beta_p)^{1/2}/\rho_o]\ \text{water}}{[(\omega P_o)^{1/2}/\rho_o]\ \text{air}} \simeq 1.14.$$

An air/water interface, therefore, provides a surprisingly good impedance match for slowly moving porous media pressure waves.

5. Radial Pressure Propagation

In this section we will assume a one-dimensional, radial geometry for the porous medium. This is the simplest model for the situation where barometric pressure fluctuations impinge on the sidewalls of an open borehole and drive pressure waves out into a permeable, horizontal layer. To be a good approximation, the layer should be much more permeable than the overlying strata to be isolated from surface pressure waves.

Starting with Eq. (9), assuming no vertical leakage ($\sigma = 0$), and using the ∇^2 operator for radial flow gives

$$\frac{\partial p}{\partial t} = \kappa\left(\frac{\partial^2 p}{\partial r^2} + \frac{1}{r}\frac{\partial p}{\partial r}\right), \tag{30}$$

where r is the radial coordinate. The region beyond the borehole radius is assumed to be semi-infinite, so that $a < r < \infty$. Again, the problem is to determine the diffusivity κ. In this case the response to fluctuations in borehole pressure is measured in a neighboring monitor hole that is sealed-off from the atmosphere.

5.1 Response to a Step Change in Pressure

As discussed in Sec. 2, one convenient method of data analysis is to represent the pressure fluctuations at the boundary by a series of step changes in pressure.

The response pressure change, $\Delta p\ (r,t)$, at radius r and time t to a boundary step change Δp_b at zero time, can be found by solving Eq. (30). The result[4] may be written

$$\Delta p\,(r,t) = \Delta p_b\, F\,(r/a, \kappa t/a^2), \tag{31}$$

where the function F is a two-parameter integral that must be evaluated by numerical integration. A computer program has been developed to carry out the numerical integration, and the details are discussed in the Appendix.

Some computed results are shown in Fig. 8, and compared with the numerical calculations of Jaeger[22] at r/a values of 2, 10, and 100. The time response in our applications is needed at values of the time parameter, $\kappa t/a^2$, that are much larger than the available tabulation. A comparison with Jaeger's tabular values shows very good agreement. A few tabular entries deviate by one unit in the third significant digit.

Figure 9 shows the time response at r/a = 50.7, which corresponds to a recent field test[23] with a borehole of 0.813-m radius and a monitor hole at a distance of 41.2 m. Also shown in Fig. 9 is the response that would be obtained in linear flow at the same distance z=r-a. A more rapid response to a step change is produced with a linear geometry.

5.2 Radial Pressure Waves

Some insight on the consequences of assuming a radial flow path geometry can be gained by making a direct comparison between monochromatic pressure waves in radial and linear flow.

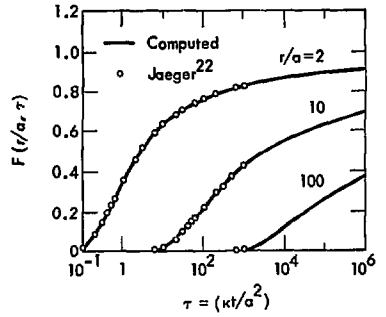

Fig. 8. Radial flow response to a unit step change at the boundary r = a.

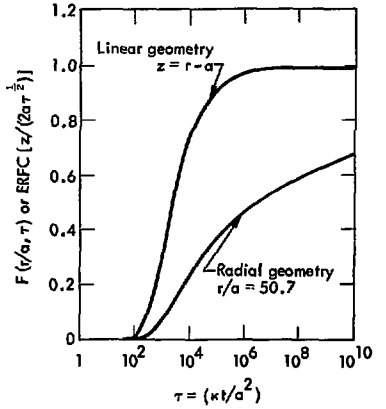

Fig. 9. Comparison of step change response in radial and linear geometry.

For radial flow, we need to solve Eq. (30) with a periodic boundary condition like Eq. (10) of Sec. 4:

$$p\,(r{=}a,t) = \varepsilon P_o \cos(\omega t).$$

The general solution, as derived in standard references[4,24] is:

$$p\,(r,t) = \varepsilon P_o \frac{N_o(\nu r)}{N_o(\nu a)} \cos\left[\omega t + \phi_o(\nu r) - \phi_o(\nu a)\right], \qquad (32)$$

where ν is the same wavenumber, $(\omega/2\kappa)^{1/2}$, defined by Eq. (21) for linear flow, and $N_o(\xi)$ and $\phi_o(\xi)$ are functions of dimensionless distance ξ. A thorough discussion of these functions is given by McLachlan[24], who also applies the theory to the penetration of temperature waves into the cylinder wall of an internal combustion engine.

If the wavenumber is large, as with high frequency waves, so that $\xi >> 1$, then Eq. (32) reduces to a form identical to Eq. (22) for linear flow except that it includes an additional factor $(r/a)^{1/2}$. A radial wave then decays faster than exponentially with distance because of the radially diverging flow, while the phase shift is the same as in linear flow.

For $\xi << 1$, the functions $N_o(\xi)$ and $\phi_o(\xi)$ are approximated[24] by:

$$N_o(\xi) \simeq -\ln(1.26\xi), \qquad (33a)$$

and

$$\phi_o(\xi) \simeq \tan^{-1}\left[\frac{\pi/4}{\ln(1.26\xi)}\right]. \qquad (33b)$$

The above equations are a good approximation for the representative field conditions used in Sec. 4.5 where wavenumber is small, $\nu = 6.79 \times 10^{-3}\ m^{-1}$ for a fluctuation with a 24-h period impinging on a 50-d porous medium.

Directly comparing radial and linear models using Eq. (32), (33), and (22), and taking r = 41.2 m and a = 0.813 m as in the last section, gives wave attenuation factors of 0.19 and 0.76, and phase lags of 112 and 63 min. If 0.19 and 112 min were the actual measured attenuation and phase lag, one could fit a linear model to the attenuation with a smaller permeability (1.4 d), but then the calculated phase lag would be way off (380 min). It appears, then, that there is sufficient difference in the functional behavior of radial and linear wave propagation to permit discrimination between these geometric models.

The larger phase lag with radial waves is a consequence of a smaller wave propagation velocity. The radial waves travel at a variable speed, starting out slowly near the origin and eventually increasing to a constant velocity $v_p = \omega/\nu$, identical to the linear wave velocity of Eq. (24). Near the origin, the wave velocity can be shown to be

$$v_p \simeq \frac{4}{\pi}\omega r \left[\ln(1.26\,\nu r)\right]^2.$$

Putting numbers into the above equation for our chosen parameter values gives 6.7 m/h at the origin r=a=0.813 m, and 14.9 m/h at r=41.2 m, as compared to the limiting wave speed of 38.5 m/h at a very large radial distance.

Conclusion

This report has explored a number of topics related to the deduction of in-situ permeability from barometric pressure fluctuations, and the main results are summarized as follows:

- The two principle methods of analysis involve decomposition of pressure fluctuations into a train of sequential rectangular pulses, or a Fourier series of sine waves. Both methods involve a superposition principle and rely on the linearity of the governing differential equation. A linearized equation, with no geometrical restrictions, has been derived to show the requirements for linearity, and the conditions under which the effect of gravity may be decoupled and neglected.
- The equations for pressure wave propagation have been shown to be identical in form to those for signal propagation on an electrical transmission line. Following the progress (velocity, amplitude, and phase shift) of a pressure wave in a dissipative porous medium offers a powerful method of visualization.
- Transmission line methods permit quantitative investigation of a number of interesting questions. This report has examined reflections from the end of a finite path, leakage to the surroundings from permeable sidewalls, and the signal perturbations introduced by a sampling probe. Leakage to the surroundings seems to be a potential source of serious error.
- Barometric pressure fluctuations have been used to investigate air-saturated porous media but may also be useful in lower permeability liquid-saturated media, such as a steeply dipping coal outcrop, because of the higher inherent diffusivity.
- A computer program has been developed and described in this report to rapidly and accurately evaluate the response in radial flow to a step change in pressure. The program is intended for use in analysis of radial pressure wave propagation from an open borehole into permeable surroundings.
- A comparison between pressure waves in radial and linear flow indicates that there are sufficient differences in attenuation and phase lag to permit discrimination between these geometric models.

Acknowledgments

I would like to acknowledge the many helpful discussions held with J. Baker on Fourier decomposition, with D. F. Snoeberger on the field measurement system, and with R. B. Rozsa on data reduction proceduros.

References

1. G. Morris and D. Snoeberger, Calculations of Pressure Change at Depth in a Nuclear Chimney following Atmospheric Pressure Change, Lawrence Livermore Laboratory, Rept. UCID-15963 (1971).
2. T. R. Butkovich and A. E. Lewis, Aids for Estimating Effects of Underground Nuclear Explosions, Lawrence Livermore Laboratory, Rept. UCRL-50929 Rev. 1 (1973).
3. H. C. Rodean, Understanding and Constructively Using the Effects of Underground Nuclear Explosions, Rev. Geophys. 6, 401 (1968).
4. H. S. Carslaw and J. C. Jaeger, Conduction of Heat in Solids (Oxford Press, 1959) 2nd. ed.
5. D. F. Snoeberger, C. J. Morris, and J. Baker, Chimney Permeability by Atmospheric Pressure Change-Instruments and Data Handling, Lawrence Livermore Laboratory, Rept. UCID-16154 (1972).
6. D. F. Snoeberger, Chimney Permeability by Atmospheric Pressure Change-Test Start-Up, Lawrence Livermore Laboratory, Rept. UCID-16110 (1972).
7. D. Snoeberger, G. Morris, and R. Rozsa, Chimney Permeability by Atmospheric Pressure Change-Preliminary Permeability Calculations, Lawrence Livermore Laboratory, Rept. UCID-16161 (1972).
8. D. F. Snoeberger, J. Baker, and C. J. Morris, Measurements and Correlation Analysis for Nuclear Chimney Permeability, Lawrence Livermore Laboratory, Rept. UCID-16302 (1973).
9. D. F. Snoeberger, C. J. Morris, and J. Baker, Data and Results, Nuclear Chimney Permeability-Test 3, Lawrence Livermore Laboratory, Rept. UCID-16436 (1974).
10. R. B. Rozsa, D. F. Snoeberger, and J. Baker, Chimney Permeability Data Analysis, Lawrence Livermore Laboratory, Rept. UCID-16440 (1974).
11. D. F. Snoeberger, J. Baker, C. J. Morris, and R. B. Rozsa, Permeability of a Nuclear Chimney and Surface Alluvium at the AEC Nevada Test Site, Lawrence Livermore Laboratory, Rept. UCID-16479 (1974).
12. D. F. Snoeberger, private communication (April, 1974).
13. G. A. Korn and T. M. Korn, Mathematical Handbook for Scientists and Engineers, (McGraw Hill, 1968).
14. Mathematical Problems in the Geophysical Sciences, W. H. Reid, Ed. (American Mathematical Society, 1971) vol. 2.
15. G. M. Jenkins and D. G. Watts, Spectral Analysis (Holden-Day, 1968).
16. R. K. Moore, Traveling-Wave Engineering (McGraw Hill, 1960).
17. R. A. Waldron, Theory of Guided Electromagnetic Waves (Van Nostrand, 1969).
18. C. W. Ulbrich, Phys. Rev. 123, 2001 (1961).
19. M. Chester, Phys. Rev. 131, 2013 (1963).
20. S. Irmay, Trans. Am. Geophys. Un. 39, 702 (1958).
21. A. E. Sherwood, Venting Model for Gas Stimulation Experiments, Lawrence Livermore Laboratory, Rept. UCID-15643 (1970).
22. J. C. Jaeger, J. Math. Phys. 34, 316 (1956).
23. R. B. Rozsa, D. F. Snoeberger, and J. Baker, Analyses of Atmospheric Pressure Response Data in Hole U9ITScU-29#2 Nevada Test Site, Lawrence Livermore Laboratory, Rept. UCID-16566 (1974).
24. N. W. McLachlan, Bessel Functions for Engineers (Oxford Press, 1955) 2nd ed.
25. Handbook of Mathematical Functions, M. Abramowitz and J. A. Stegun, Eds. (National Bureau of Standards, AMS-55, 1964).

Appendix – Radial Flow Integral

Consider the function $F(\xi,\tau)$ defined by

$$F(\xi,\tau) = \int_0^\infty g(\xi,\tau,u)\,du, \tag{A1}$$

where the integrand $g(\xi,\tau,u)$ is defined by

$$g(\xi,\tau,u) = \frac{2}{\pi}(1 - e^{-\tau u^2})\,h(\xi,u), \tag{A2}$$

and the function $h(\xi,u)$ is defined by

$$h(\xi,u) = \frac{J_0(u)\,Y_0(\xi u) - Y_0(u)\,J_0(\xi u)}{u[J_0^2(u) + Y_0^2(u)]}, \tag{A3}$$

where J_0 and Y_0 are the usual notations for zero order Bessel functions of the first and second kind, and u is a dummy variable of integration.

The two-parameter radial flow integral $F(\xi,\tau)$ is the solution to the differential equation of diffusion (heat flow, linearized gas flow, slightly compressible liquid flow, etc.) for the semi-infinite region bounded internally at $\xi=1$, where the region is initially at zero and where the cylindrical boundary surface is held at unity, in relative temperature or pressure units, for $\tau>0$[4]. Dimensionless distance and time parameters ξ and τ are defined by

$$\xi = r/a, \tag{A4}$$

and

$$\tau = \kappa t/a^2, \tag{A5}$$

where r is radial distance, a is the inner boundary radius, and κ is the diffusivity (thermal or mass as appropriate to the physical situation being modeled) with units of $[r^2t^{-1}]$, e.g. $[m^2s^{-1}]$.

Numerical Evaluation of $F(\xi,\tau)$

The radial flow integral, Eq. (A1), must be evaluated, in general, by numerical integration unless τ is either very small or very large as discussed below. A computer subroutine has been developed to carry out the integration automatically.

The subroutine is called with specified values of ξ and τ, and is designed to evaluate F with an absolute error magnitude of $|\epsilon|< 10^{-3}$, and usually with error in the 10^{-4} range or smaller. This error estimate holds for any value of τ and for $2 \geq \xi \geq 100$. The error may be somewhat larger for ξ either very large or very close to 1.0. The computer time required is about 2s/integration or less on the CDC-7600 computer.

Because of the complicated nature of the integrand, it is convenient to break the region of integration over the dummy variable u into four parts,

$$F = F_1 + F_2 + F_3 + F_4, \tag{A6}$$

where the limits of integration for the four integrals above depend on the input parameters ξ and τ:

F_1: $0 \leq u < u_{min}(\tau)$,

F_2: $u_{min}(\tau) \leq u < u_{mid}(\tau)$,

F_3: $u_{mid}(\tau) \leq u < u_{max}(\xi)$,

and

F_4: $u_{max}(\xi) \leq u < \infty$.

The philosophy has been to develop a fast subroutine for the situation where a value of the parameter ξ is specified and the integral F is then required for many successive values of the parameter τ, with τ increasing from some small value, close to zero, to a much larger value, perhaps about τ[8].

The integrals will be discussed in the order in which they are evaluated on entering the subroutine, F_4, F_3, F_1, and F_2.

The Integral $F_4(\xi)$

The integration range $u_{max} \to \infty$ is covered by F_4, where u_{max} is set sufficiently large such that F_4 can be evaluated analytically. For large u, the exponential term in Eq. (A2) may be neglected and

$$g(\xi,\tau,) \simeq \frac{2}{\pi}\,h(\xi,u). \tag{A7}$$

From the properties of the Bessel function, J_0 and Y_0 at large values of the argument u, it follows that

$$h(\xi,u) \simeq \frac{\sin[(\xi-1)u]}{\sqrt{\xi}\,u}, \tag{A8}$$

and therefore

$$F_4(\xi) = \frac{2}{\pi\sqrt{\xi}} \int_{u_{max}}^\infty \frac{\sin[(\xi-1)u]}{u}\,du + \epsilon_4, \tag{A9}$$

where ϵ_4 is the integral error as a result of approximating g and h as given above. We find from numerical experimentation that

setting $u_{max} = 10^2\,\xi^{-1/2}$ will keep error ϵ_4 of the order of 10^{-4}, and that this error is insenitive to τ.

The integral in Eq. (A9) is simply related to the well-known sine integral, for which as accurate analytical approximation exists,[25] and therefore $F_4(\xi)$ may be evaluated when the parameter ξ is specified. It is not necessary to recalculate F_4 on subsequent calls to the subroutine, provided the input value of ξ is unchanged.

The Integral $F_3(\xi,\tau)$

Using Simpson's Rule with an integration step size of 0.001 in u, both F_3 and F_2 are evaluated numerically. The Bessel functions in Eq. (A3) are represented by accurate polynomial approximations.[25] The only distinction lies in the limits of integration. The lower limit of F_3, u_{mid}, is set such that

$$e^{-\tau u_{mid}^2} = 10^{-4}$$

which gives, on solving for u_{mid},

$$u_{mid} = 3.04\,\tau^{-1/2}.$$

The limit above allows the exponential term to be dropped from the integrand, as in Eq. (A7). This in turn permits faster integration of F_3 and also means that F_3 need not be recalculated on subsequent calls to the subroutine, assuming a sequence of calls involving increasing values of the parameter τ. When the input τ value has increased by a factor of 10, u_{mid} is reevaluated and the limits of F_3 and F_2 are readjusted.

The Integral $F_1(\xi,\tau)$

The integrand $g(\xi,\tau,u)$ is well behaved at the origin (u=0), in the sense that $g \to 0$ as $u \to 0$. However, the integrand rises very steeply near the origin, especially if τ is large. One can show that the first turning point (maximum in g) occurs at a value of u that is essentially independent of ξ and given by

$$u_t \simeq \sqrt{\frac{1.25}{\tau}}.$$

Therefore a large value of τ ($\sim 10^6$) requires a step size much smaller than 0.001 to accurately represent the integrand near the origin. The procedure followed in the subroutine is to use an integration step size for F_1 equal to $u_t/10.0$, but no larger than 0.001, and to carry the integration out to:

$$u_{min} = 100\,u_t.$$

The Integral $F_2(\xi,\tau)$

The integral F_2 is evaluated last in the sequence. The lower limit (u_{min}) is set by the upper limit of F_1, and the upper limit (u_{mid}) is set by the lower limit of F_3, as previously discussed. The integration step size is the same as F_3, 0.001.

Small τ Approximation

If τ is small enough, the integral $F(\xi,\tau)$ may be approximated[4] analytically by

$$F(\xi,\tau) \simeq \frac{\mathrm{erfc}\,(y)}{\sqrt{\xi}}, \qquad \text{(A10)}$$

where erfc (y) is the complementary error function of y, with y defined by

$$y = \frac{\xi - 1}{2\sqrt{\tau}}.$$

The criterion specified in the subroutine is to evaluate F from Eq. (A10) when:

$$y \geq 3.0.$$

Large τ Approximation

If τ is large enough, the integral $F(\xi,\tau)$ is approximated analytically by

$$F(\xi,\tau) \simeq 1 - \frac{2\ln\xi}{\ln(4\tau) - 2\gamma_E}\left\{1 - \frac{\gamma_E}{\ln(4\tau) - 2\gamma_E}\right\}, \qquad \text{(A11)}$$

where $\gamma_E = 0.57722...$ is Euler's constant. The criterion specified for the use of Eq. (A11) is when $\tau \geq 10^8$.